

*Original scientific paper*

## ENHANCING ECO-EFFICIENT LABORATORY-SCALE STEEL PRODUCTION VIA INNOVATIVE PROCESS AND EQUIPMENT DESIGN WITH CIRCULAR RESOURCE UTILIZATION

Emre Alan

ÇEMTAŞ Çelik Mak. San. ve Tic. A. Ş., R&D Center

### ABSTRACT

This study presents the development of an eco-efficient laboratory-scale production route for long steel products, focusing on sustainable casting and hot deformation processes. Conventional casting using 80x80 mm molds and gravity filling generated significant shrinkage defects, leading to scrap generation, repeated melting, and reduced material efficiency. Alternative mold designs with a 15° inclination and exothermic feeders were evaluated via simulation software, minimizing defects and enabling Ø70 mm castings with 20% less raw material. A new laboratory-scale hot rolling unit replaced hydraulic presses, achieving the target Ø29 mm round cross-section in a single cycle with a 0.83 reduction ratio, increasing specimen yield and reducing energy consumption. Equipment selection prioritized the reuse of idle industrial motors and gearboxes, aligning with circular economy principles. Mechanical testing and microstructural outcomes obtained from the new process were closer to industrial production standards, demonstrating not only enhanced process yields but also improved product quality. Overall, the combined process modifications reduced scrap, minimized energy use, and leveraged existing resources, demonstrating a practical, sustainable and eco-friendly approach for laboratory-scale steel production.

**Keywords:** steel; laboratory-scale productions; process optimization; energy-efficient processing

Corresponding Author:

Emre Alan,  
ÇEMTAŞ Çelik Mak. San. ve Tic. A.Ş. / R&D Center  
AOS Bulvarı, No.3, 16140 Nilüfer, Bursa, Türkiye  
Tel.: +90555 508 0700  
E-mail address: emre48@gmail.com

### 1. INTRODUCTION

The properties of steel materials can be tailored by modifying their chemical composition and heat treatment parameters. Accordingly, numerous studies focus on developing innovative steels with enhanced performance. However, industrial-scale production for new product development is often limited by cost, labor, and time constraints. In such cases, laboratory-scale experiments provide a significant advantage by allowing the identification of optimal solutions.

Nevertheless, laboratory-scale studies must accurately reflect the outcomes of industrial-scale productions. For this purpose, different equipment and process setups are employed. The equipment used in laboratory-scale physical simulations of steel production processes may either be small-scale versions of the corresponding industrial processes or alternative setups that allow investigation of process outputs. For instance, Aula et al. [1] developed a laboratory-scale physical model of the electric arc furnace (EAF) used for melting

scrap steel. This setup also enables studies on direct reduced iron (DRI) production, which is particularly relevant for sustainable steelmaking. In other studies, induction melting systems have been used to produce molten steel [2,3], focusing solely on achieving the molten steel without replicating the oxidizing conditions present in EAF processes.

For continuous casting research, dynamic water models are commonly used to simulate tundish operations. While commercially available solutions from traditional technology suppliers exist at various scales, some researchers utilize custom-designed equipment [4-6]. For physical modeling of plastic deformation processes such as rolling and forging, commercially available thermal-mechanical simulators are widely employed [7-9]. These commercial systems provide significant advantages for investigating the effects of different parameters in hot deformation processes, allowing precise observation of material behavior. However, the sample sizes are generally insufficient for subsequent tests or industrial applications, and the high investment cost, along with outsourcing service fees, often limits their accessibility. Alternatively, in laboratory-scale production studies requiring larger sample sizes, high-capacity equipment such as forging presses is often employed [10, 11]. Since these machines are typically part of industrial production lines, direct access is not always possible, and implementing the necessary modifications for specific research purposes can be challenging. Furthermore, acquiring such equipment as a dedicated laboratory unit would require substantial financial investment.

While the above approaches have advanced understanding of individual processes, this study aims to enable practical integration of these processes within a complete laboratory-scale production chain through efficient equipment and process improvements, rather than relying directly

on commercialized equipment, which is often costly and limits broader applicability. Unlike prior studies that primarily focus on single operations, the present work addresses improvements across the entire sequence encompassing melting, casting, and hot deformation for laboratory-scale production of long steel products. Key contributions include the development of innovative mold designs for gravity casting, the introduction of a new hot rolling unit to replace hydraulic presses, and the strategic reuse of idle industrial equipment. These enhancements not only increase production efficiency by means of sustainable production and product quality but also align with circular economy principles by extending the service life of existing resources and reducing investment costs.

## **2. MATERIALS AND METHODS**

### **2.1. Laboratory-scale melting and casting operations**

In the process with the existing laboratory setup, steel materials were melted and cast using a conventional induction melting system. Industrially produced hot-rolled steels were charged to the system as the raw material and melted together with predetermined amounts of ferroalloy additions to achieve the desired chemical composition.

Since the steel materials used in laboratory-scale production are typically produced on an industrial scale via vacuum degassing, melting, and casting operations are conducted within a vacuum cabinet under vacuum pressure to prevent the re-oxidation of the molten metal and maintain the cleanliness of the steel.

In the current laboratory-scale casting process, the molten steel is transferred from the induction melting unit into a permanent mold using a method which is generally known as "gravity casting". During the casting operation, the molten steel is poured from a set height, hitting the mold's interior walls and filling the mold cavity, which

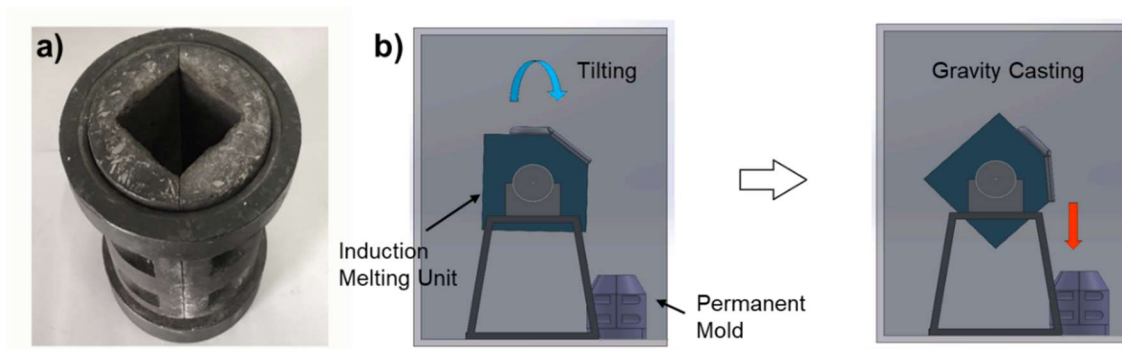


**Figure 1.** a) Permanent mold with 80x80 mm square cross-section used in laboratory-scale casting, b) schematic illustration of the gravity casting process

generates turbulent flow and leads to the formation of casting defects. Additionally, because the upper part of the mold also served as the pouring basin and remained open, the molten metal in this region did not come into contact with the mold during solidification. Consequently, heat transfer in this area occurred differently, creating a temperature gradient between the upper part of the mold and the regions in direct contact with the molten steel. As a result of the chosen casting method and current mold design during the mold filling and solidification stages, significant shrinkage cavities and porosity-related casting defects were observed. The ingot casting mold with an 80x80 mm square cross-section and the casting method used in the current laboratory production route are shown in Figure 1.

In the processes carried out with the existing casting mold and method, the casting defects observed after solidification are shown in Figure 2. Before hot deformation, the necessary inspections are

performed on the cast products, and sections containing defects are removed by cutting. In these productions, a significant portion of the castings were scrapped, particularly due to shrinkage cavities. Moreover, when the required minimum casting dimension for subsequent hot rolling could not be achieved after cutting and defect removal, re-production was necessary.

In the casting of metallic materials, "counter-gravity" filling methods are often preferred to minimize casting defects [12,13]. Since mold designs in this method incorporate modifications such as the pouring basin, cavity, runners, risers, and pouring gates, the molds tend to be larger in size [14,15]. However, in the current setup, the limited space available within the vacuum cabinet restricts the application of the counter-gravity filling method. Therefore, alternative mold designs were developed using the existing equipment and casting method to reduce casting defects.

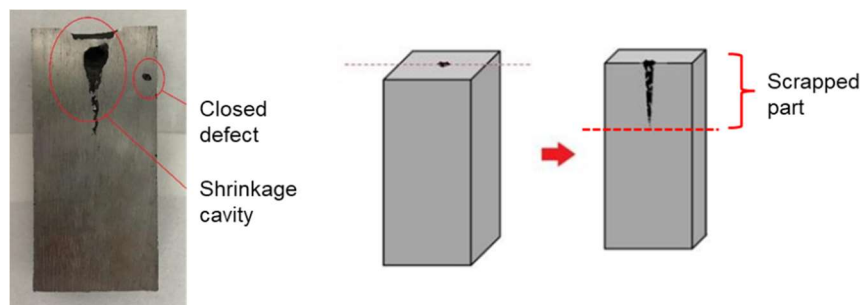


**Figure 2.** Typical casting defects observed in products obtained using the existing 80x80 mm cross-section mold and gravity casting method

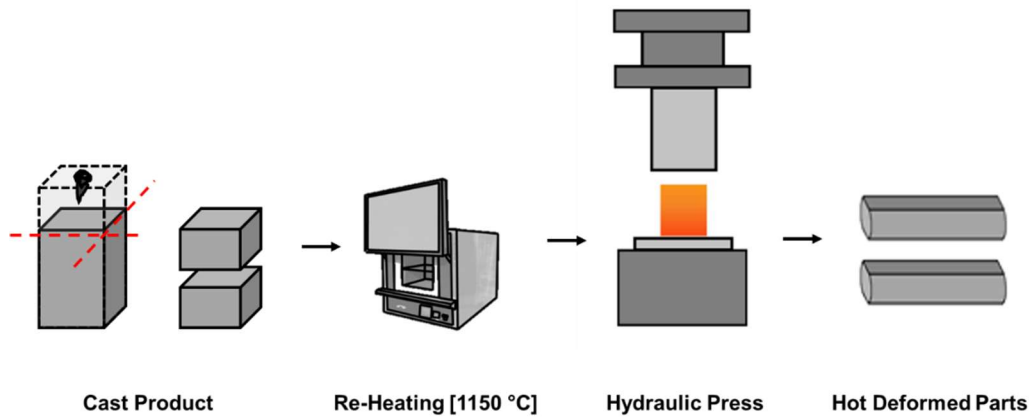


**Figure 3.** Flow diagram of the former laboratory-scale productions.

Studies have indicated that molds with inclined designs can reduce turbulence-related defects in gravity casting [16,17]. Based on these findings, molds with inclination angles of 5°, 15°, and 25° were designed to produce castings with a round cross-section of Ø70 mm and a length of 250 mm. To further enhance casting quality, exothermic feeders were incorporated into the molds to prevent shrinkage defects. NovaCast simulations were conducted on these designs to identify the most efficient configuration.

## 2.2. Laboratory-scale hot deformation process

The process route illustrated in Figure 3 represents the method previously employed in laboratory-scale operations before implementing the improvements described in this study. The solidified cast products with an 80x80 mm square cross-section, trimmed to remove casting defects, were deformed using hydraulic presses to achieve dimensions suitable for mechanical testing, with a required sample length of 180 mm. Due to the limited capacity of the hydraulic presses and heat loss from the material during processing, the heating and deformation steps had to be repeated three times to reach the target dimensions. This procedure increased both energy consumption and the time required for labor and equipment use.

In order to improve process efficiency and material yield during hot deformation, a new laboratory-scale rolling unit was developed to substitute the hydraulic presses. The unit was designed using equipment that had either completed its service life or was no longer active in the industrial production line, aiming to utilize existing materials sustainably and contribute to the principles of the circular economy.

The aim of the hot deformation via the new hot rolling unit was to produce hot-rolled final products with a Ø29 mm round cross-section. Since the initial cast material was expected to have a Ø70 mm round cross-section, the rolling was planned to be performed using round-to-oval pass transitions to achieve the desired final dimensions. During this process, the material elongates along the rolling direction while spreading laterally, resulting in an oval cross-section at the end of each pass. Shinokura and Takai [18] proposed the following formula to calculate the maximum spreading width in rolling operations with round-to-oval caliber transitions.

$$W_{max} = W_i \left( 1 + \gamma \frac{\sqrt{R(H_{is} - H_{0s})} A_h}{W_i + 0.5H_i A_0} \right) \quad (1)$$

where  $W_{max}$  represents the maximum spreading and  $W_i$  denotes the width of the

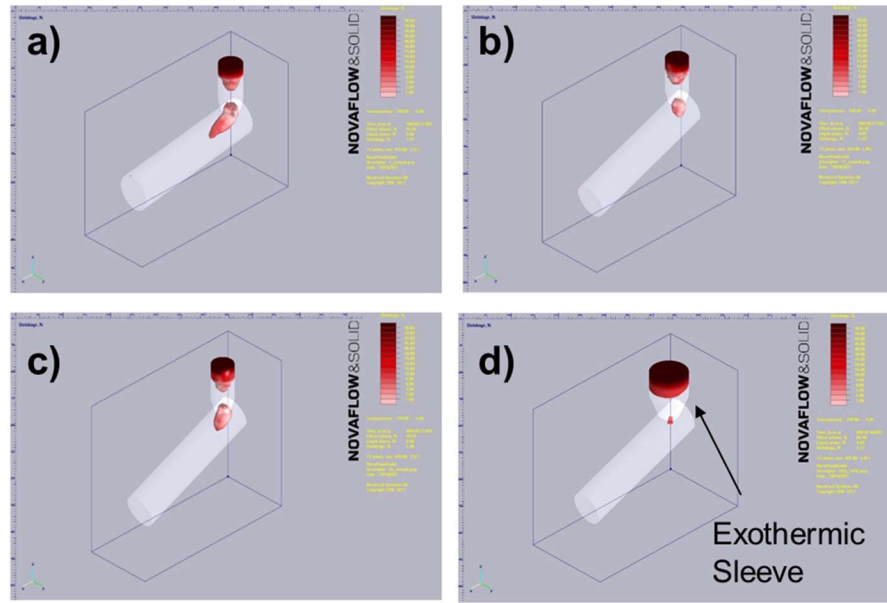


**Figure 4.** Simulation results for inclined casting mold designs: (a) 5°, (b) 15°, (c) 25°, and (d) 15° with exothermic sleeve.

material being rolled.  $A_0$  is the cross-sectional area of the initial material, and  $A_h$  corresponds to the cross-sectional area after deformation,  $R$  indicates the radius of the roller, and  $H$  represents the height of the round and oval cross-section geometries.

The rolling unit was designed to consist of a pair of rollers, an electric motor, a gearbox, a motor driver, the external frame, and additional accessories. The electric motor and gearbox capacities necessary to achieve hot rolling at the designated dimensions were estimated through calculations using multiple models.

The mechanical properties and microstructural features of the steels produced using the newly designed

production route were evaluated and compared with those obtained from the conventional production route.

### 3. RESULTS

#### 3.1. Design and optimization of casting molds

Figure 4 presents the results of modelling and simulation studies for casting mold designs with different inclination angles.

Analysis of defect formation indicated that the mold with a 15° inclination provided the most effective solution. Furthermore, the addition of an exothermic feeder significantly mitigated shrinkage cavity formation. Based on these findings, the

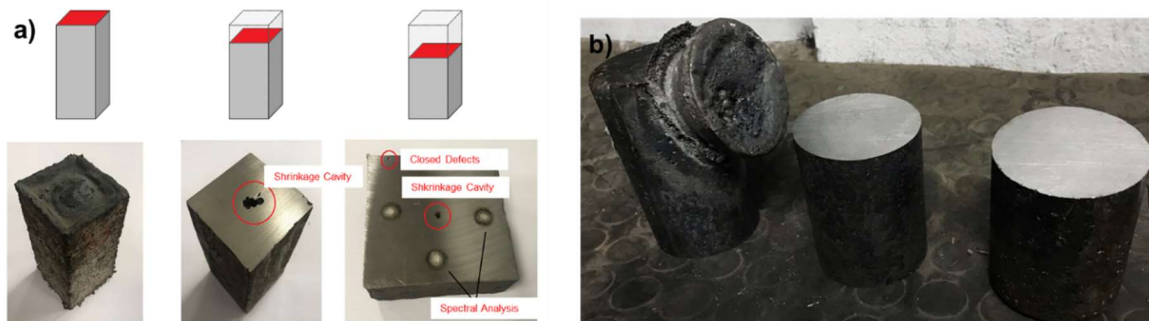


**Figure 5.** Comparison of macrostructural investigations of laboratory-scale cast produced with a) existing mold and b) newly designed mold.

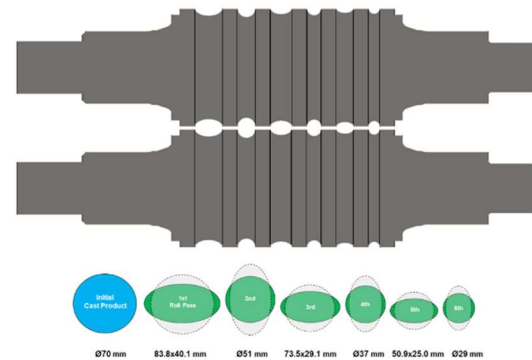
mold design with a 15° inclination incorporating an exothermic feeder was selected for physical production.

Figure 5 presents the macrostructural evaluation of laboratory-scale productions carried out with both the new and existing molds. The results show that the use of the new molds substantially reduced casting defects during solidification compared to the existing molds. Consequently, scrap due to casting defects and the need for re-production were decreased, indicating improvements in both product quality and energy efficiency. The newly designed molds enabled the production of castings with the target Ø70 mm round cross-section using 8 kg of raw material, compared to 10 kg in the conventional process, representing a 20% improvement in raw material utilization. In addition, the melting time was reduced from 33 to 27 minutes, yielding an 18.2% increase in efficiency for the induction melting system, which relies on electrical energy.

### 3.2. Development and implementation of a newly designed hot rolling unit

Based on the dimensions of the rollers used in the laboratory-scale hot rolling unit, as shown in Figure 6, it was determined that hot-rolled bars with a target Ø29 mm cross-section could be produced from Ø70 mm material after six rolling passes, with approximately 35% deformation applied per pass. The resulting bars were calculated to have a length of approximately 1460 mm after hot rolling.

The rolling load and torque for each roll-pass were calculated using the mathematical model developed by El-Bitar et al. [19]. During hot deformation, the material, preheated to 1150 °C, was expected to remain above 920 °C after processing. Cooling simulations indicated that the rolling operation needed to be completed within 50 seconds to maintain the target temperature.



**Figure 6.** Round-to-oval roller caliber configuration for six-pass hot rolling of Ø70 mm to cast Ø29 mm.

As the material's cross-section decreased and its length increased after each pass, the roller rotational speed had to be increased to ensure that the longer material could be processed within the allotted time for each pass. For the six-pass rolling process, designed to be completed within the desired rolling time, the required roller speeds for each pass were calculated and are presented in Table 1.

The calculation results of total torque and rolling loads based on the designated pass schedule, roller width, rolling speed, and

**Table 1.** Calculated hot rolling process parameters for each rolling pass

Roll Pass No.	Roller radius [mm]	Time [s]	Rotational speed [rpm]	Velocity of the workpiece [mm/s]
1. Roll Pass	139.4	3.5	5.8	85.3
2. Roll Pass	128.5	4.5	7.2	97.4
3. Roll Pass	150.4	4.5	7.9	125.1
4. Roll Pass	142.5	5.0	9.2	137.9
5. Roll Pass	154.5	6.0	11.0	178.6
6. Roll Pass	150.0	6.5	11.8	217.5



material temperature are presented in Figure 7. Assuming a gearbox efficiency of 85%, the maximum torque was predicted to occur during the second roll pass, reaching 28.8 kNm. Accordingly, a gearbox with a capacity exceeding 33.9 kNm was selected to ensure sufficient performance.

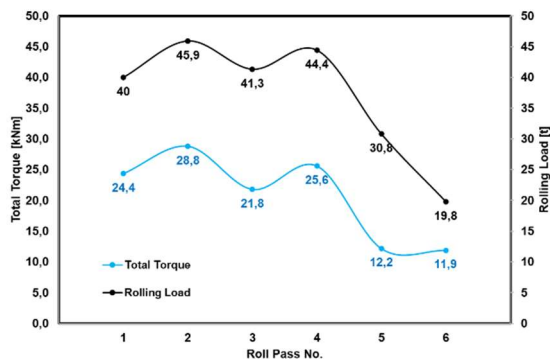


**Figure 7.** Calculated total torque and rolling loads along the designated pass schedule for the hot rolling unit

Investigations were carried out on the 37 kW, 45 kW, and 55 kW electric motors that were currently idle at the facility and

available for potential use in the laboratory-scale hot rolling unit. According to the calculations presented in Table 2, operating the 37 kW motor at its nominal 50 Hz frequency would not achieve the desired rotational speed of 11.8 rpm. Calculations indicated that, with a 35 kNm torque gearbox, the desired roller speed of 12.3 rpm at 50 Hz on the output shaft could be achieved using either the 45 kW or the 55 kW motor. However, a compatible drive unit was available only for the 45 kW motor, which led to its selection for the laboratory-scale hot rolling unit.

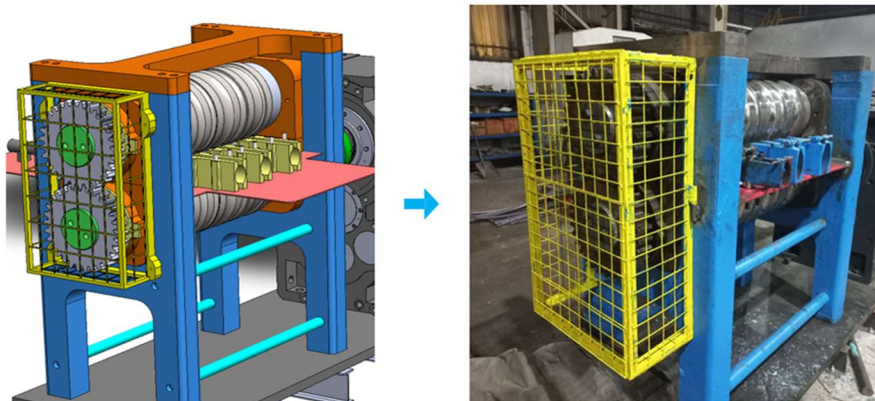
Figure 8 shows the laboratory-scale hot rolling unit assembled using the equipment selected based on the calculations.

Figure 9 shows a schematic comparison of the current process route and the new laboratory-scale process route incorporating the newly developed equipment.

In the previous production route, achieving the minimum specimen length of 180 mm for mechanical testing required repeating the heating and deformation process three

**Table 2.** Calculated electric motors and corresponding gearbox parameters for the laboratory-scale hot rolling unit

Electric Motor Parameters				Reducer Parameters	
Power [kW]	Frequency [Hz]	Speed [rpm]	Moment [kNm]	Torque [kNm]	Speed [rpm]
37	50	1500	0.236	35.0	10.1
45	50	1500	0.287	35.0	12.3
55	50	1500	0.350	35.0	15.0



**Figure 8.** Newly designed laboratory-scale hot rolling unit.

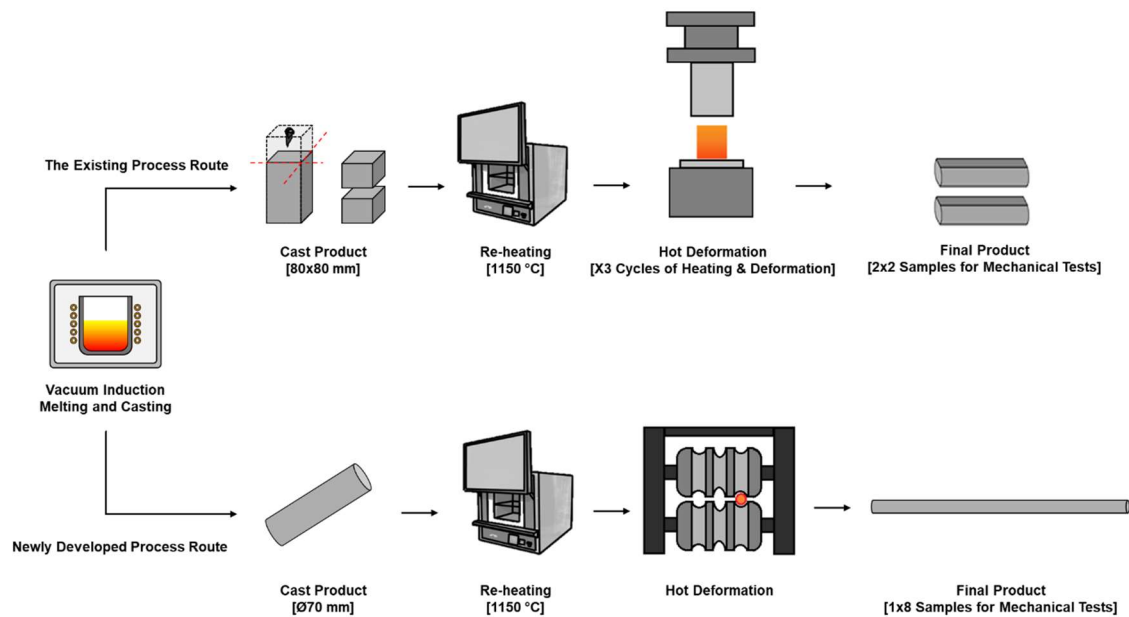


**Figure 9.** Comparison of the existing and improved laboratory-scale process routes with newly developed equipment

times, resulting in a reduction ratio of 0.64. With the newly developed equipment, the same requirement was met in a single cycle, increasing the reduction ratio to 0.83, corresponding to a 30% improvement. After removal of shrinkage cavities, the previous route produced only four specimens, whereas the new route allowed the production of 1460 mm bars, increasing the specimen count to eight. Furthermore, reducing the raw material requirement from 10 kg to 8 kg improved the specimen yield per kilogram of input material by 150%.

### 3.3. Evaluation of Mechanical Properties

Mechanical tests were conducted at room temperature following standard procedures. Tensile tests were performed on cylindrical specimens in accordance with DIN 50125 [20], having a gauge length of 50 mm and a diameter of 10 mm. Charpy impact tests were carried out on standard V-notched specimens in accordance with ISO 148-1 [21], with nominal dimensions of 10x10x55 mm. For each condition, three specimens were tested and the reported results represent average values. All tests were performed using a Zwick Z400 universal testing machine and a Roell Amsler RKP450 impact tester.

**Table 3.** Comparison of the mechanical properties of samples obtained from existing and newly developed laboratory-scale production routes

The Production Route	Yield Strength [MPa]	Tensile Strength [MPa]	Elongation [MPa]	Impact Energy* [J]
Industrial Scaled Productions	764	1256	16.3	21.3
Laboratory Scaled The Existing Process	717	1188	12.4	15.3
Laboratory Scaled The Newly Developed Process	755	1261	16.0	20.7

\* 2 mm-V notched samples, Room temperature.



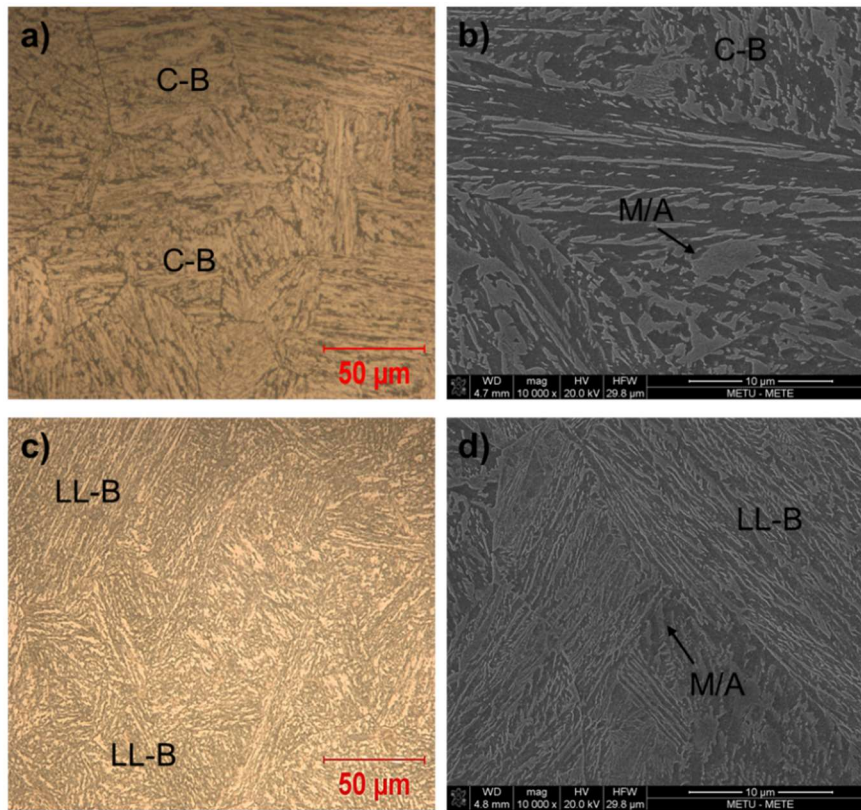


**Figure 10.** Comparison of microstructures from laboratory-scale productions; (a, c) OM and (b, d) SEM images of samples produced with existing and newly designed processes, respectively (C-B: coarser bainite, LL-B: lath-type bainite, M/A: martensite/austenite islands)

Table 3 summarizes the mechanical test results obtained using both the conventional and the newly developed production routes. When compared with industrial production data, the outcomes of the new process route exhibit a closer agreement with industrial values. This trend aligns with previous reports in the literature, where increased reduction ratios were identified as a key factor contributing to improved mechanical properties, particularly with respect to impact toughness [22].

### 3.4 Microstructural Characterization

Optical microscopy (OM) and scanning electron microscopy (SEM) images of the laboratory-scale productions are presented in Figure 10. In the samples that were hot rolled and subsequently air-cooled, the microstructures were predominantly composed of bainite. The samples subjected

to multiple reheating cycles with lower reduction ratios exhibited coarser bainitic (C-B) morphologies with relatively larger martensite/austenite (M/A) islands. In contrast, the new production route resulted in microstructures dominated by lath-type bainite (LL-B) with finer M/A formations. These microstructural variations were found to influence strength and toughness in a manner consistent with literature reports [23-25].

### 4. CONCLUSIONS

This study demonstrated that laboratory-scale steel production can be significantly enhanced through eco-efficient process and equipment design. By adopting inclined mold designs tailored to gravity casting, casting defects were minimized and scrap was reduced. These changes not only improved raw material utilization but also decreased melting time and lowered energy

consumption. The replacement of hydraulic presses with a newly developed hot rolling unit enabled more efficient deformation in a single cycle, increasing reduction ratios and overall material efficiency.

Additionally, the integration of reused components, including rolling mill rolls, electrical motors, gearboxes, controller units, and rollers, demonstrated a sustainable design approach aligned with circular economy principles, prolonging equipment lifespan and reducing investment costs for new machinery. Mechanical testing and microstructural investigations confirmed that the properties achieved via the new process route were much closer to industrial-scale results, validating improvements in both process efficiency and product quality.

Overall, the combination of optimized mold design, efficient hot rolling, and strategic reuse of existing equipment provides a practical, cost-effective, and eco-friendly framework for laboratory-scale steel production. The results highlight that sustainable production can be achieved without compromising material performance, offering a model for future laboratory-scale prototyping in steel manufacturing.

### Conflicts of Interest

The authors declare no conflict of interest.

### REFERENCES

- [1] M. Aula, H. Pauna, T. Kokkonen, V.-V. Visuri. Laboratory-scale EAF. In Proc. Adv. Steels *Green Planet Seminar*, University of Oulu: Oulu, Finland, (2024) pp. 1–10. <https://doi.org/10.13140/RG.2.2.24264.02565>
- [2] X. Zhang, J. Li, L. Yan, L., & X. He, Effect of film-like retained austenite on low temperature toughness of high strength offshore steel, *Materials Research Express*, 6(2019) 11, 116530 <https://doi.org/10.1088/2053-1591/ab445c>
- [3] Y. Huang, X. Jin, & G. Cai, Evolution of microstructure and mechanical properties of a new high-strength steel containing Ce element, *Journal of Materials Research*, 32(2017) 20, 3894–3903 <https://doi.org/10.1557/jmr.2017.382>
- [4] B. Bul'ko, M. Molnár, P. Demeter, D. Baricová, A. Pribulová, P. Futáš, Study of the Influence of Intermix Conditions on Steel Cleanliness. *Metals*, 8 (2018), 852 <https://doi.org/10.3390/met8100852>
- [5] X. Zhi, W. Biao, L. Zhao-yi, J. Guang-lin, Dynamic Water Modeling and Application of Billet Continuous Casting. *J. Iron Steel Res. Int.* 15 (2008), pp. 14–17 [https://doi.org/10.1016/S1006-706X\(08\)60023-0](https://doi.org/10.1016/S1006-706X(08)60023-0)
- [6] B. Konar, D. Li, K. Chattopadhyay, Demystifying the CC Mold at the University of Toronto: The First Full-Scale Mold Water Model in North American Academia, In Proc. *Iron & Steel Technol. Conf. (AISTech 2019)*, Pittsburgh, USA, 2019, pp. 1331–1344
- [7] A. Kozłowska, S. Sławski, W. Borek, A. Grajcar. Physical and Numerical Investigation of Hot Deformation Behavior in Medium-Mn Steel for Automotive Forgings. *Mater.*, 18 (2025), p. 1883 <https://doi.org/10.3390/ma18081883>
- [8] E. Alan, Effect of Prior Deformation on Microstructural Evolution and Retained Austenite Stability in Bainite–Martensite Structures of Continuously Cooled Low-Carbon Steel, *Eur. Mech. Sci.*, 9 (2025), pp. 291–301 <https://doi.org/10.26701/ems.1726120>
- [9] L.A. Dobrzański, W. Borek, M. Czaja, J. Mazurkiewicz, Structure of X11MnSiAl17-1-3 Steel after Hot-Rolling and Gleeble Simulations, *Arch. Mater. Sci. Eng.*, 61 (2013), pp. 13–21.
- [10] M. Ackermann, B. Resiak, P. Buessler, B. Michaut, & W. Bleck, Effect of molybdenum and cooling regime on microstructural heterogeneity in bainitic steel wires, *Steel research international*, 91 (2020) 11, 1900663.
- [11] C. Feng, B. Bai & Y. K. Zheng, Effect of 0.06% Nb on the microstructure and mechanical properties of Mn-series low carbon air-cooling bainitic steels, *Advanced Materials Research*, 284 (2011), pp. 1191–1195 <https://doi.org/10.4028/www.scientific.net/AMR.284-286.1191>
- [12] J. Campbell, Sixty Years of Casting Research. *Metall. Mater. Trans. A*, 46 (2015), pp. 4848–4853 <https://doi.org/10.1007/s11661-015-2955-8>

- [13] D. Du, J. An, A. Dong & B. Sun, A review of the progress and challenges of counter-gravity casting, *Journal of Materials Science & Technology*, 216 (2025), pp. 1-26  
<https://doi.org/10.1016/j.jmst.2024.07.037>
- [14] K. Herfurth, S. Scharf. Casting, In Springer Handb. Mech. Eng.; Springer International Publishing: Cham, Switzerland, 2021, pp. 325–356.
- [15] J. Campbell, Castings Practice: The Ten Rules of Castings; Elsevier: Amsterdam, The Netherlands, 2004.
- [16] H. Wang, G. Djambazov, K.A. Pericleous, R.A. Harding, M. Wickins, Modelling the Dynamics of the Tilt-Casting Process and the Effect of the Mould Design on the Casting Quality. *Comput. Fluids*, 42 (2011), pp. 92–101, <https://doi.org/10.1016/j.compfluid.2010.11.010>
- [17] L. F. Pease, J. Bao, R. Safarkoolan, T. G. Veldman, N. R. Phillips, P. S. McNeff, C. K. Clayton, Flow Obstacles Minimize Surface Turbulence in Tilt Casting, *Chem. Eng. Sci.*, 230 (2021), 230, 116104  
<https://doi.org/10.1016/j.ces.2020.116104>
- [18] T. Shinokura, K. Takai, A New Method for Calculating Spread in Rod Rolling, *J. Appl. Metalwork*, 2 (1982), pp. 94–99  
<https://doi.org/10.1007/BF02834206>
- [19] T. El-Bitar, M. El-Meligy, E. El-Shenawy, Prediction of Roll Separating Force in a Roll Pass Design of Micro-Alloyed Steel Rods, *High Perform. Optimum Design Struct. Mater.*, 137 (2014), pp. 67–79.  
<https://doi.org/10.2495/HPSM140071>
- [20] Deutsches Institut für Normung (DIN), DIN 50125: Metallische Werkstoffe – Zugversuch von Prüfkörpern – Abmessungen und Form, Beuth Verlag, Berlin, 2016
- [21] International Organization for Standardization (ISO), ISO 148-1: Metallic materials – Charpy impact test – Part 1: Test method, ISO, Geneva, 2016
- [22] H. S. Kim, M. Kang, M. Park, B. J. Kim, Y. S. Kim, T. Y. Lee, ... Y. S. Ahn, Effects of Hot Rolling Reduction on Microstructural Evolution and Mechanical Properties of 1.25 Cr-1Mo-0.5 V-0.3 C Steel for High-Speed Rail Brake Discs, *Arch. Metall. Mater.*, 69 (2024)  
<https://doi.org/10.24425/amm.2024.147797>
- [23] F. Y. Küçükakarsu, İ. İ. Ayhan, E. Alan, D. Taştēmür, S. Gündüz, Effect of Hot Rolling Process Parameters on the Microstructure and Mechanical Properties of Continuously Cooled Low-Carbon High-Strength Low-Alloy (HSLA) Steel., *Mater. Test.*, 64 (2022), pp. 1136–1149  
<https://doi.org/10.1515/mt-2021-2220>
- [24] İ. İ. Ayhan, C. Güney, E. Alan, A. Bal, M. F. Kayadeğirmeni, F. Y. Küçükakarsu, ... S. Gündüz, The Influence of Multi-Pass Hot Rolling Parameters and Subsequent Heat Treatment on Microstructure and Mechanical Properties of Medium-Carbon Steel., *Trans. Indian Inst. Met.*, 77 (2024), pp. 3475–3485  
<https://doi.org/10.1007/s12666-024-03401-0>
- [25] E. Alan, İ. İ. Ayhan, B. Ögel, D. Uzunsoy. A Comparative Assessment of Artificial Neural Network and Regression Models to Predict Mechanical Properties of Continuously Cooled Low Carbon Steels: An External Data Analysis Approach, *J. Innov. Eng. Nat. Sci.*, 4 (2024), pp. 495–513  
<https://doi.org/10.61112/jiens.1445518>